Journal of Sound and Vibration (1999) **219**(2), 279–306
Article No. jsvi.1998.1873, available online at http://www.idealibrary.com.on IDEAL

FINITE ELEMENT COMPUTATION OF THREE-DIMENSIONAL ELASTOACOUSTIC VIBRATIONS

A. Bermúdez, L. Hervella-Nieto
Departamento de Matemática Aplicada, Universidade de Santiago de Compostela, Spain

AND

R. Rodríguez
Departamento de Ingeniería Matemática, Universidad de Concepción, Chile

(*Received* 17 *September* 1997, *and in final form* 16 *July* 1998)

In this paper, the interior elastoacoustic problem in a 3D domain is solved. Displacement variables are used for both the fluid and the solid. To avoid the typical spurious modes of this formulation, a non-standard discretization is used, consisting of classical linear tetrahedral finite element for the solid and Raviart–Thomas elements of lowest order for the fluid. A new unknown is introduced on the interface between solid and fluid to impose the transmission conditions.

1. INTRODUCTION

The computation of the motion of an elastic solid interacting with a fluid is an important problem which occurs in many engineering applications. During the last few years, a large amount of work has been devoted to this subject. A general overview can be found in the monogaphs by Morand and Ohayon [1] and Conca *et al*. [2], where numerical methods and further references are also given.

This paper deals with a particular fluid–solid interaction: the *elastoacoustic problem*. It is concerned with the determination of the small amplitude vibration modes of an elastic structure containing an ideal compressible fluid (see Figure 1). In this case, the displacements are small enough to produce a linear response of the structure. An homogeneous fluid is considered and the effects of gravity are neglected. Also other usual simplifications in this kind of problem are adopted, namely, that the fluid velocities are small enough so that the convective effects can be neglected, and that the viscous effects in the fluid are not relevant (see, for instance, the book by Zienkiewicz and Taylor [3]).

The problem of determining the vibration of a fluid alone is usually treated by choosing the pressure as the primary variable [4]. However, for coupled systems, such a choice leads to non-symmetric eigenvalue problems [3] whose

0022–460X/99/020279 + 28 $30.00/0

computational solution involves considerable complications. Because of this, the fluid part has been alternatively described by different variables: for instance, Everstine [5] has used the velocity potential, obtaining a quadratic eigenvalue problem; Morand and Ohayon [6] have used both the pressure and the displacement potential, obtaining a symmetric problem.

Several authors have used primitive variable formulations (i.e., displacements in both fluid and solid), for example, in frequency calculations and response spectrum analysis, because they do not require any special interface conditions or new solution strategies. This approach could be applied to the solution of a broad range of problems (in particular non-linear ones) [7, 8] and leads to sparse symmetric matrices. However a serious drawback of this formulation was pointed out several years ago by Kiefling and Feng [9]: they showed that it suffers from the presence of spurious circulation modes, with no physical entity, when the displacement in the fluid is discretized by standard finite elements.

Since then several approaches have been proposed to avoid this drawback. Hamdi *et al*. [10] introduced an irrotational constraint by means of a penalty method. This technique does not attain the complete elimination of spurious modes, but they are pushed towards higher frequencies and therefore do not appear among the first modes. This fact was theoretically justified by Bermúdez and Rodríguez [11]. However, Olson and Bathe [12] demonstrated that the method "locks up" in the frequency analysis of a solid vibrating in a fluid cavity. They also showed that reduced integration performed on the penalty formulation yields some improvement in results but does not ensure solution convergence in a general case.

On the other hand, Chen and Taylor [13] proposed a four-node element with reduced integration in the stiffness matrix of the fluid combined with a projection

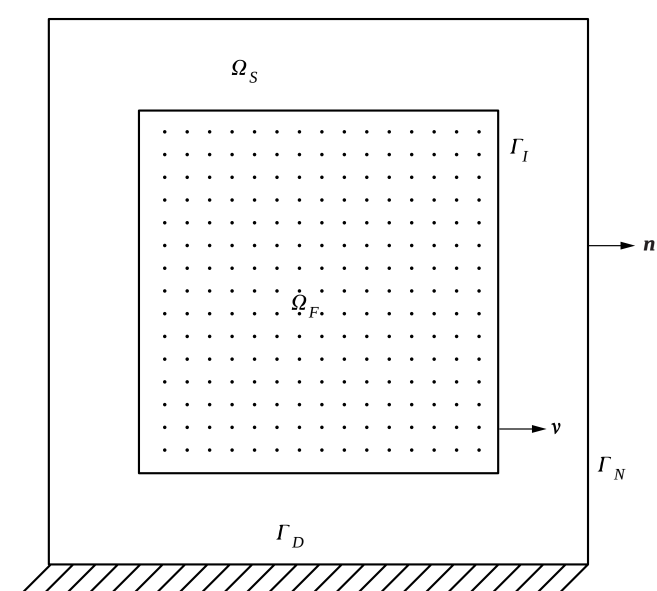

Figure 1. Fluid and solid domains in 2D.

on the element mass matrix. Numerical experiments show that this method is useful to eliminate spurious modes but, up to now, no theoretical analysis has been performed.

More recently, Bermúdez *et al*. [11, 14] introduced an alternative approach. It consists of using different finite element spaces for the solid and the fluid. For two-dimensional problems, standard three-node triangles are used for the solid, whereas so-called "edge elements" are chosen for the fluid displacements. These "edge elements", introduced by Raviart and Thomas [15], are incomplete linear polynomials; their degrees of freedom are located at the edges of the triangles and represent the constant normal components of the displacement field along them. Non-existence of spurious modes has been mathematically proved in reference [14], whereas numerical tests showing the good performance of the method are provided in reference [11].

In both the above mentioned papers, the method is applied to two-dimensional problems, which implies an important limitation for practical applications. On the other hand, as remarked by Wang and Bathe [8] the coupling in this approach needs special considerations because of the fact that the degrees of freedom of the fluid elements are not those of the structure.

In this paper, a variant of this method avoiding this drawback is presented and it is tested with numerical experiments over different three-dimensional examples. This variant consists of introducing a new variable, the pressure on the fluid–solid interface, which allows the coupling kinematic condition to be imposed in a simpler way. Furthermore, this methodology would allow incompatible meshes to be used on the interface (i.e., meshes on the fluid and the solid domain not necessarily matching on the common boundary).

The outline of the paper is as follows. In section 2 the spectral problem to be solved is stated along with a weak symmetric formulation involving the displacements in both, the fluid and the solid and the interface pressure. In section 3 the finite element method is introduced and the main theoretical results concerning error estimates and non-existence of spurious eigenmodes are summarized. In section 4 the problem is written in matrix form and it is shown that it is a well posed generalized eigenvalue problem. Finally, in section 5, numerical results for some 3D test examples are given in order to validate the proposed methodology.

2. STATEMENT OF THE PROBLEM

Ω_F and Ω_S denote the three-dimensional interior and exterior domains, occupied by the fluid and the solid, respectively. The exterior boundary of Ω_S is the union of two parts, Γ_D and Γ_N, the structure being fixed on Γ_D. $\mathbf{n}$ denotes the normal exterior vector along Γ_N, Γ_I denote the interface between the solid and the fluid, and $\boldsymbol{\nu}$ is its unit normal vector pointing outwards Ω_F. Figure 1 shows corresponding two-dimensional domains for a better understanding of the notation.

If an external force $\mathbf{F}$ is applied on Γ_N, the equations describing the motion of the coupled system can be written in the following way [1]:

$$\sum_{j=1}^{3} \frac{\partial \sigma_{ij}(\mathbf{w})}{\partial x_j} = \rho_s \frac{\partial^2 w_i}{\partial t^2} \quad \text{in} \quad \Omega_S, \quad i = 1, 2, 3,$$

$$-\frac{\partial p}{\partial x_i} = \rho_F \frac{\partial^2 u_i}{\partial t^2} \quad \text{in} \quad \Omega_F, \quad i = 1, 2, 3,$$

$$p = -\rho_F c^2 \operatorname{div} \mathbf{u} \quad \text{in} \quad \Omega_F, \qquad \mathbf{u} \cdot \mathbf{v} = \mathbf{w} \cdot \mathbf{v} \quad \text{on} \quad \Gamma_I,$$

$$\sigma(\mathbf{w})\mathbf{v} = -p\mathbf{v} \quad \text{on} \quad \Gamma_I, \qquad \mathbf{w} = \mathbf{0} \quad \text{on} \quad \Gamma_D, \qquad \sigma(\mathbf{w})\mathbf{n} = \mathbf{F} \quad \text{on} \quad \Gamma_N.$$

In the above expressions $x = (x_1, x_2, x_3)$ are the co-ordinates of a material point either in the solid or in the fluid; $p(x)$ is the fluid pressure; $\mathbf{w}(x) = (w_1, w_2, w_3)$ and $\mathbf{u}(x) = (u_1, u_2, u_3)$ are the displacement vectors of the solid and the fluid, respectively; $\operatorname{div} \mathbf{u} = \Sigma_{j=1}^{3} \partial u_j / \partial x_j$ is the divergence of the fluid displacement field; $\sigma(\mathbf{w})$ is the stress tensor in the structure which (upon assuming a linear isotropic elastic material) is related to the solid displacements $\mathbf{w}$ by Hooke's law [16]:

$$\sigma_{ij}(\mathbf{w}) = \frac{E v_s}{(1 + v_s)(1 - 2v_s)} \sum_{k=1}^{3} \varepsilon_{kk}(\mathbf{w})\delta_{ij} + \frac{E}{1 + v_s} \varepsilon_{ij}(\mathbf{w}), \qquad i, j = 1, 2, 3,$$

where $\varepsilon_{ij}(\mathbf{w}) = \frac{1}{2}(\partial w_i / \partial x_j + \partial w_j / \partial x_i)$ is the linear strain tensor, E is the Young modulus and v_S the Poisson ratio of the structure; finally ρ_F and ρ_S are the respective densities and c is the sound speed in the fluid.

For determining the free vibration modes of the coupled system, no exterior forces are considered and harmonic pressure and motions are looked for: i.e.,

$$\mathbf{F}(x, t) = \mathbf{0}, \quad x \in \Gamma_N \qquad p(x, t) = P(x)\, \mathrm{e}^{\mathrm{i}\omega t}, \quad x \in \Omega_F,$$

$$\mathbf{u}(x, t) = \mathbf{U}(x)\, \mathrm{e}^{\mathrm{i}\omega t}, \quad x \in \Gamma_F, \qquad \mathbf{u}(x, t) = \mathbf{W}(x)\, \mathrm{e}^{\mathrm{i}\omega t}, \quad x \in \Omega_S,$$

ω being the angular frequency of the mode. By replacing these expressions into the above equations, the following eigenvalue problem is obtained.

Find an angular frequency ω and amplitudes of pressure and displacement fields P, $\mathbf{U}$ and $\mathbf{W}$, not all identically zero, satisfying

$$-\sum_{j=1}^{3} \frac{\partial \sigma_{ij}(\mathbf{W})}{\partial x_j} = \omega^2 \rho_s W_i \quad \text{in} \quad \Omega_S, \quad i = 1, 2, 3, \tag{1}$$

$$\frac{\partial P}{\partial x_i} = \omega^2 \rho_F U_i \quad \text{in} \quad \Omega_F, \quad i = 1, 2, 3, \tag{2}$$

$$P = -\rho_F c^2 \operatorname{div} \mathbf{U} \quad \text{in} \quad \Omega_F, \qquad \mathbf{U} \cdot \mathbf{v} = \mathbf{W} \cdot \mathbf{v} \quad \text{on} \quad \Gamma_I, \tag{3, 4}$$

$$\sigma(\mathbf{W})\mathbf{v} = -P\mathbf{v} \quad \text{on} \quad \Gamma_I, \qquad \mathbf{W} = \mathbf{0} \quad \text{on} \quad \Gamma_D, \qquad \sigma(\mathbf{W})\mathbf{n} = \mathbf{0} \quad \text{on} \quad \Gamma_N. \tag{5–7}$$

To give a variational formulation of problem (1–7), equation (1) is integrated multiplied by a virtual solid displacement $\mathbf{Z}$ satisfying the Dirichlet condition (6) and Green's formula is used to obtain

$$\int_{\Omega_s} \sigma(\mathbf{W}):\varepsilon(\mathbf{Z})\,\mathrm{d}x + \int_{\Gamma_I} \sigma(\mathbf{W})\mathbf{v}\cdot\mathbf{Z}\,\mathrm{d}\Gamma = \omega^2 \int_{\Omega_S} \rho_s \mathbf{W}\cdot\mathbf{Z}\,\mathrm{d}x.$$

Then equation (2) is integrated multiplied by a virtual fluid displacement $\mathbf{Y}$ and Green's formula and equation (3) are used to obtain

$$\int_{\Omega_F} \rho_F c^2 \operatorname{div}\mathbf{U} \operatorname{div}\mathbf{Y}\,\mathrm{d}x + \int_{\Gamma_I} P\mathbf{Y}\cdot\mathbf{v}\,\mathrm{d}\Gamma = \omega^2 \int_{\Omega_F} \rho_F \mathbf{U}\cdot\mathbf{Y}\,\mathrm{d}x.$$

Now, by adding both equations and using equation (5) one has

$$\int_{\Omega_F} \rho_F c^2 \operatorname{div}\mathbf{U} \operatorname{div}\mathbf{Y}\,\mathrm{d}x + \int_{\Omega_S} \sigma(\mathbf{W}):\varepsilon(\mathbf{Z})\,\mathrm{d}x + \int_{\Gamma_I} P(\mathbf{Y}\cdot\mathbf{v} - \mathbf{Z}\cdot\mathbf{v})\,\mathrm{d}\Gamma$$

$$= \omega^2\left(\int_{\Omega_F} \rho_F \mathbf{U}\cdot\mathbf{Y}\,\mathrm{d}x + \int_{\Omega_S} \rho_s \mathbf{W}\cdot\mathbf{Z}\,\mathrm{d}x\right).$$

Finally, the kinematic constraint (4) between both displacement fields is imposed in a weak way by integrating this equation multiplied by any test function Q defined on Γ_I:

$$\int_{\Gamma_I} Q(\mathbf{U}\cdot\mathbf{v} - \mathbf{W}\cdot\mathbf{v})\,\mathrm{d}\Gamma = 0.$$

All together one obtains the following spectral hybrid problem.

Find an angular frequency ω, *displacement fields* $\mathbf{U}:\Omega_F\to\mathbb{R}^3$ *and* $\mathbf{W}:\Omega_S\to\mathbb{R}^3$ *and interface pressure* $P:\Gamma_I\to\mathbb{R}$, *with* $\mathbf{U}$, $\mathbf{W}$ *and* P *not all identically zero*, *satisfying*

$$\int_{\Omega_F} \rho_F c^2 \operatorname{div}\mathbf{U} \operatorname{div}\mathbf{Y}\,\mathrm{d}x + \int_{\Omega_S} \sigma(\mathbf{W}):\varepsilon(\mathbf{Z})\,\mathrm{d}x + \int_{\Gamma_I} P(\mathbf{Y}\cdot\mathbf{v} - \mathbf{Z}\cdot\mathbf{v})\,\mathrm{d}\Gamma$$

$$= \omega^2\left(\int_{\Omega_F} \rho_F \mathbf{U}\cdot\mathbf{Y}\,\mathrm{d}x + \int_{\Omega_S} \rho_S \mathbf{W}\cdot\mathbf{Z}\,\mathrm{d}x\right), \qquad \forall(\mathbf{Y},\mathbf{Z})\in\chi, \tag{8}$$

and

$$\int_{\Gamma_I} Q(\mathbf{U}\cdot\mathbf{v} - \mathbf{W}\cdot\mathbf{v})\,\mathrm{d}\Gamma = 0, \qquad \forall Q\in\mathscr{P}. \tag{9}$$

In the first equation,

$$\sigma(\mathbf{W})::\varepsilon(\mathbf{Z}) = \sum_{i,j=1}^{3} \sigma_{ij}(\mathbf{W})\varepsilon_{ij}(\mathbf{Z})$$

is the standard inner product of second order tensors and

$$\chi = \{(\mathbf{Y}, \mathbf{Z}):\mathbf{Y}:\Omega_F \to \mathbb{R}^3 \quad \text{and} \quad \mathbf{Z}:\Omega_S \to \mathbb{R}^3 \quad \text{with} \quad \mathbf{Z} = \mathbf{0} \quad \text{on} \quad \Gamma_D\}$$

is the set of pairs of virtual displacements. In the second one, $\mathscr{P}$ is the set of arbitrary functions $Q:\Gamma_I \to \mathbb{R}$.

Note that equation (9) imposes the kinematic constraint (4) on any solution of this problem. Denote by $\mathscr{V}$ the set of kinematically admissable virtual displacements (i.e., those satisfying this constraint):

$$\mathscr{V} = \{(\mathbf{Y}, \mathbf{Z}) \in \chi : \mathbf{Y} \cdot \mathbf{v} = \mathbf{Z} \cdot \mathbf{v} \quad \text{on} \quad \Gamma_I\}.$$

Then, any solution of the hybrid spectral problem (8, 9) also provides a solution of the following pure displacement eigenvalue problem.

Find an angular frequency ω *and a pair of displacements* $(\mathbf{U}, \mathbf{W}) \in \mathscr{V}$, *with* $\mathbf{U}$ *and* $\mathbf{W}$ *not both identically zero*, *satisfying*

$$\int_{\Omega_F} \rho_F c^2 \operatorname{div} \mathbf{U} \operatorname{div} \mathbf{Y} \, \mathrm{d}x + \int_{\Omega_S} \sigma(\mathbf{W}):\varepsilon(\mathbf{Z}) \, \mathrm{d}x$$

$$= \omega^2 \left(\int_{\Omega_F} \rho_F \mathbf{U} \cdot \mathbf{Y} \, \mathrm{d}x + \int_{\Omega_S} \rho_S \mathbf{W} \cdot \mathbf{Z} \, \mathrm{d}x \right), \qquad \forall (\mathbf{Y}, \mathbf{Z}) \in \mathscr{V}, \tag{10}$$

As it is typical in displacement formulations, $\omega = 0$ is an eigenfrequency of this problem (and consequently of problem (8, 9)) with an infinite-dimensional eigenspace

$$\mathscr{K} = \{(\mathbf{U}, \mathbf{0}) \in \chi : \operatorname{div} \mathbf{U} = 0 \quad \text{in} \quad \Omega_F \quad \text{and} \quad \mathbf{U} \cdot \mathbf{v} = 0 \quad \text{on} \quad \Gamma_I\}.$$

These eigenmodes consist of pure rotational fluid motions inducing neither vibrations in the solid nor variations of pressure in the fluid. They are mathematical solutions of the eigenproblem with no physical entity. They do not correspond to vibration modes of the coupled system, but they arise because no irrotational constraint is imposed to the fluid displacements.

The rest of the eigenfrequencies of problem (8, 9) are strictly positive and correspond to actual vibrations of the coupled fluid–solid system. The whole spectrum of the problem can be characterized by using the spectral theorem for compact operators and the fact that the fluid displacements associated with $\omega = 0$ are orthogonal to any irrotational fluid displacement (i.e., those of the form

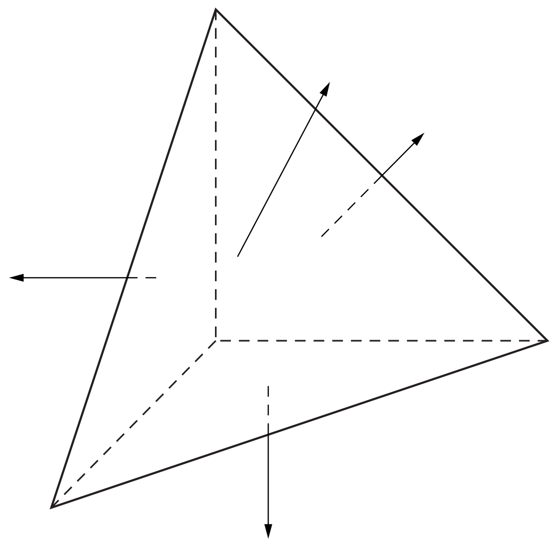

Figure 2. Raviart–Thomas finite element.

$\mathbf{U} = \mathbf{grad}\, \phi$, for some potential ϕ). In fact, the following result, proved in reference [18], yields:

The solutions of problem (8, 9) *are* $\omega = 0$ *and a sequence of strictly positive eigenfrequencies of finite multiplicity* $\omega_1, \omega_2, \ldots, \omega_n, \ldots$ *converging to* ∞. *The set of eigenmodes of* $\omega = 0$ *consists of pure rotational motions of the fluid*, *whereas those of* $\omega_1, \omega_2, \ldots, \omega_n, \ldots$ *are irrotational on the fluid*.

3. FINITE ELEMENT DISCRETIZATION

In spite of the fact that problems (8, 9) and (10) are mathematically equivalent, from the computational point of view it is much simpler to deal with the first one. We are going to solve this problem by using a finite element discretization. Consider regular partitions in tetrahedra of Ω_F and Ω_S. Let h denote the mesh size of both "triangulations".

The simplest method consists of using classical four-node tetrahedral elements for each component of both displacements (i.e., continuous functions which are linear on each tetrahedron, their degrees of freedom being the displacements at the vertices of the mesh). However, this is not a suitable choice since spurious modes arise when such a discretization is used [9, 10].

As stated above, zero frequency eigenmodes of the continuous problem (8, 9) fill an infinite dimensional subspace of circulation fluid motions with no physical entity. Therefore, the finite elements to be used should lead to a discrete problem having zero as an eigenvalue with a large enough associated eigenspace consisting of discrete rotational fluid motions. Otherwise, spurious modes with non-zero frequencies placed among the physical ones would arise polluting the numerical results. This is what happens, for instance, when standard finite elements are used for the fluid displacements.

Instead, the lowest order Raviart–Thomas elements [15] are used for the displacement field in the fluid $\mathbf{U}_h$ (see Figure 2). These elements consist of vector valued functions which are incomplete linear polynomials of the form

$$\mathbf{U}_h(x) = (a + dx_1, b + dx_2, c + dx_3), \qquad a, b, c, d \in \mathbb{R},$$

when restricted to each tetrahedron.

These polynomial functions have constant normal components on any plane of the space. In fact, consider a general plane of equation $\alpha x_1 + \beta x_2 + \gamma x_3 = \delta$ with coefficients normalized such that $\alpha^2 + \beta^2 + \gamma^2 = 1$. Then $\mathbf{n} = (\alpha, \beta, \gamma)$ is its unit normal vector and, for any point (x_1, x_2, x_3) in this plane, we have

$$\begin{aligned}\mathbf{U}_h(x_1, x_2, x_3) \cdot \mathbf{n} &= \alpha(a + dx_1) + \beta(b + dx_2) + \gamma(c + dx_3)\\ &= \alpha a + \beta b + \gamma c + (\alpha x_1 + \beta x_2 + \gamma x_3)d\\ &= \alpha a + \beta b + \gamma c + \delta d,\end{aligned}$$

which is a constant independent of the point (x_1, x_2, x_3) of the plane.

In particular these fields have constant normal components on each of the four faces of the tetrahedron. Moreover, the values of these constants define a unique polynomial function of this type. To see this, let the equations of the four planes defining a tetrahedron be given by

$$\alpha_i x_1 + \beta_i x_2 + \gamma_i x_3 = \delta_i, \qquad i = 1, \ldots, 4, \tag{11}$$

with $\alpha_i^2 + \beta_i^2 + \gamma_i^2 = 1$ as above. The problem is to find four numbers a, b, c, d such that

$$(a + dx_1)\alpha_i + (b + dx_2)\beta_i + (c + dx_3)\gamma_i = V_i, \tag{12}$$

where V_i, $i = 1, \ldots, 4$, are arbitrarily prescribed values. By using equation (11), the linear system (12) becomes

$$\begin{aligned}\alpha_1 a + \beta_1 b + \gamma_1 c + \delta_1 d &= V_1\\ \alpha_2 a + \beta_2 b + \gamma_2 c + \delta_2 d &= V_2\\ \alpha_3 a + \beta_3 b + \gamma_3 c + \delta_3 d &= V_3\\ \alpha_4 a + \beta_4 b + \gamma_4 c + \delta_4 d &= V_4\end{aligned}.$$

Since all planes have to be "independent" (i.e., any two of them cannot be parallel), this system has a unique solution.

The global discrete displacement field $\mathbf{U}_h$ is allowed to have discontinuous tangential components on the faces of the tetrahedra of the triangulation but its (constant) normal components must be continuous through these faces, these constant values being its degrees of freedom. Because of this, div $\mathbf{U}_h$ is globally well defined on Ω_F.

For each component of the displacements in the solid, standard four-node tetrahedral elements are used.

Finally, the interface pressure is discretized by means of piecewise constant functions.

So, let

$$\chi_h = \{(\mathbf{Y}_h, Z_h) : \mathbf{Y}_h \text{ Raviart–Thomas},$$
$$\mathbf{Z}_h \text{ four-node tetrahedral} \quad \text{and} \quad \mathbf{Z}_h|_{\Gamma_D} = \mathbf{0}\},$$

and let $\mathscr{P}_h$ be the space of functions defined on Γ_I which are constant on each face of the triangulation on the interface. We have the following discrete hybrid problem.

Find a real number ω_h, *a pair of displacements* $(\mathbf{U}_h, \mathbf{W}_h) \in \chi_h$ *and an interface pressure* $P_h \in \mathscr{P}_h$, *with* $\mathbf{U}_h$, $\mathbf{W}_h$ *and* P_h *not all identically zero, satisfying*

$$\int_{\Omega_F} \rho_F c^2 \operatorname{div} \mathbf{U}_h \operatorname{div} \mathbf{Y}_h \, \mathrm{d}x + \int_{\Omega_S} \sigma(\mathbf{W}_h) : \varepsilon(\mathbf{Z}_h) \, \mathrm{d}x + \int_{\Gamma_I} P_h (\mathbf{Z}_h \cdot \mathbf{v} - \mathbf{Y}_h \cdot \mathbf{v}) \, \mathrm{d}\Gamma$$

$$= \omega_h^2 \left(\int_{\Omega_F} \rho_F \mathbf{U}_h \cdot \mathbf{Y}_h \, \mathrm{d}x + \int_{\Omega_S} \rho_S \mathbf{W}_h \cdot \mathbf{Z}_h \, \mathrm{d}x \right), \qquad \forall (\mathbf{Y}_h, \mathbf{Z}_h) \in \chi_h, \tag{13}$$

and

$$\int_{\Gamma_I} Q_h (\mathbf{W}_h \cdot \mathbf{v} - \mathbf{U}_h \cdot \mathbf{v}) \, \mathrm{d}\Gamma = 0, \qquad \forall Q_h \in \mathscr{P}_h. \tag{14}$$

Equation (14) imposes weakly the kinematic constraint on the discrete displacements. By using in this equation a test function Q_h taking the value 1 on a particular face $\mathscr{F}$ on the interface Γ_I and vanishing on all the other faces, one has

$$\int_{\mathscr{F}} (\mathbf{U}_h \cdot \mathbf{v} - \mathbf{W}_h \cdot \mathbf{v}) \, \mathrm{d}\Gamma = 0. \tag{15}$$

From this equation it is deduced that, in general, the normal components $\mathbf{U}_h \cdot \mathbf{v}$ and $\mathbf{W}_h \cdot \mathbf{v}$ do not coincide on the whole Γ_I. Indeed, the Raviart–Thomas finite elements used for the fluid displacements have constant per face normal components, whreas those of the four-node elements used in the solid are linear. Then equation (15) implies that both coincide only at the barycenter M of each face $\mathscr{F} \subset \Gamma_I$. In fact,

$$[\mathbf{U}_h(M) \cdot \mathbf{v}] \text{ area } (\mathscr{F}) = \int_{\mathscr{F}} \mathbf{U}_h \cdot \mathbf{v} \, \mathrm{d}\Gamma = \int_{\mathscr{F}} \mathbf{W}_h \cdot \mathbf{v} \, \mathrm{d}\Gamma = [\mathbf{W}_h(M) \cdot \mathbf{v}] \text{ area } (\mathscr{F}),$$

the latter because the barycenter rule is exact for linear functions.

Let us remark that $\omega_h = 0$ is an eigenfrequency of the discrete problem (13, 14) and the set of its associated eigenmodes is $\mathscr{K}_h = \mathscr{K} \cap \chi_h$, which provides a good approximation of the eigenspace $\mathscr{K}$ of $\omega = 0$ in the continuous problem (see reference [18]). In this reference, the following approximation result has also been proved under reasonable hypotheses on the regularity of the three-dimensional domains.

Let $\omega_1 \leqslant \omega_2 \leqslant \cdots \leqslant \omega_n \leqslant \cdots$ *and* $\omega_{h1} \leqslant \omega_{h2} \leqslant \cdots \leqslant \omega_{hN_h}$ *be the strictly positive eigenfrequencies of the continuous and the discrete problems*, *respectively* (*in both cases repeated as many times as their multiplicity*). *Then there exists a constant* r *between* 0 *and* 1 *such that*

$$|\omega_n - \omega_{hn}| \leqslant Ch^{2r}.$$

This property shows, in particular, that no spurious mode can arise. Moreover, the nth strictly positive eigenfrequency of the discrete problem approximates that of the continuous one with an error of order h^{2r}, which depends on the geometry of both domains, Ω_F and Ω_S. Let us remark that, for instance, for a convex fluid domain, the constant r determining the order of convergence is the same as that for the computation of the vibration modes of the structure *in vacuo* by using classical four-node linear elements.

4. MATRICIAL DESCRIPTION

In the previous section, a discrete formulation of our problem has been stated. Now, a matricial description of it is given and it is shown that it is a well posed symmetric generalized eigenvalue problem involving sparse matrices.

For the sake of simplicity, meshes for the solid and the fluid are considered, which are compatible on the interface. However, it is important to notice that this is not at all a requirement of the method. Indeed, the interface pressure P could be discretized by using a triangulation on the interface independent of the fluid and solid meshes.

Let us call $\tilde{\mathbf{U}}_h$, $\tilde{\mathbf{W}}_h$, $\tilde{\mathbf{P}}_h$, $\tilde{\mathbf{Y}}_h$ and $\tilde{\mathbf{Z}}_h$ the vectors of nodal components of $\mathbf{U}_h$, $\mathbf{W}_h$, P_h, $\mathbf{Y}_h$ and $\mathbf{Z}_h$, respectively. The matrices associated with the bilinear forms in the variational formulation are defined by

$$\tilde{\mathbf{Z}}_h^t K_S \tilde{\mathbf{W}}_h = \int_{\Omega_S} \sigma(\mathbf{W}_h):\varepsilon(\mathbf{Z}_h)\,\mathrm{d}x, \qquad \tilde{\mathbf{Z}}_h^t M_S \tilde{\mathbf{W}}_h = \int_{\Omega_S} \rho_s \mathbf{W}_h \cdot \mathbf{Z}_h\,\mathrm{d}x,$$

$$\tilde{\mathbf{Y}}_h^t K_F \tilde{\mathbf{U}}_h = \int_{\Omega_F} \rho_F c^2 \operatorname{div} \mathbf{U}_h \operatorname{div} \mathbf{Y}_h\,\mathrm{d}x \qquad \tilde{\mathbf{Y}}_h^t M_F \tilde{\mathbf{U}}_h = \int_{\Omega_F} \rho_F \mathbf{U}_h \cdot \mathbf{Y}_h\,\mathrm{d}x,$$

$$\tilde{\mathbf{Z}}_h^t C \tilde{\mathbf{P}}_h = \int_{\Gamma_I} P_h \mathbf{Z}_h \cdot \mathbf{v}\,\mathrm{d}\Gamma, \qquad \tilde{\mathbf{Y}}_h^t D \tilde{\mathbf{P}}_h = \int_{\Gamma_I} P_h \mathbf{Y}_h \cdot \mathbf{v}\mathrm{d}\Gamma.$$

K_S and M_S are the standard stiffness and mass matrices of the solid, respectively; K_F and M_F are the corresponding ones for the fluid. Notice that the order of the two latter is $N_F \times N_F$, with N_F being the total number of faces of the fluid mesh; moreover they are highly sparse because only a maximum of seven entries per row can be different from zero (this corresponds to the number of faces of two adjacent tetrahdedra).

On the other hand, C and D are the coupling matrices of the interface pressure with the solid and the fluid, respectively. Both are very sparse too. Indeed D is an $N_F \times N_I$ rectangular matrix, with N_I being the number of faces on the fluid-solid interface. Each column of D has exactly only one non-zero entry. To describe more precisely the structure of this matrix assume for simplicity that the degrees of fredom in the fluid are numbered in such a way that the first N_I ones correspond to the faces on the interface. Then

$$D = \begin{bmatrix} d_1 & & \\ & \ddots & \\ & & d_{N_I} \\ & & \\ & 0 & \end{bmatrix},$$

with d_i being the area of the ith face.

Similarly, C is an $N_S \times N_I$ rectangular matrix, with N_S being the number of degrees of freedom of the solid mesh. Each column of C has at most nine non-zero entries because this is the number of degrees of freedom at each face of the solid.

Problem (13, 14) is written in terms of these matrices in the following way:

$$\begin{pmatrix} K_S & 0 & C \\ 0 & K_F & D \\ C^t & D^t & 0 \end{pmatrix} \begin{pmatrix} \tilde{\mathbf{W}}_h \\ \tilde{\mathbf{U}}_h \\ \tilde{\mathbf{P}}_h \end{pmatrix} = \omega_h^2 \begin{pmatrix} M_S & 0 & 0 \\ 0 & M_F & 0 \\ 0 & 0 & 0 \end{pmatrix} \begin{pmatrix} \tilde{\mathbf{W}}_h \\ \tilde{\mathbf{U}}_h \\ \tilde{\mathbf{P}}_h \end{pmatrix}.$$

Both matrices in this eigenvalue problem are singular; however, by performing a translation in the eigenvalues, it can be written in an equivalent more convenient way:

$$\begin{pmatrix} K_S + M_S & 0 & C \\ 0 & K_F + M_F & D \\ C^t & D^t & 0 \end{pmatrix} \begin{pmatrix} \tilde{\mathbf{W}}_h \\ \tilde{\mathbf{U}}_h \\ \tilde{\mathbf{P}}_h \end{pmatrix} = (1 + \omega_h^2) \begin{pmatrix} M_S & 0 & 0 \\ 0 & M_F & 0 \\ 0 & 0 & 0 \end{pmatrix} \begin{pmatrix} \tilde{\mathbf{W}}_h \\ \tilde{\mathbf{U}}_h \\ \tilde{\mathbf{P}}_h \end{pmatrix}. \tag{16}$$

As we show below, the matrix on the left hand side is now non-singular and, consequently, it yields a well posed generalized eigenvalue problem. Furthermore, both matrices of this problem are symmetric and highly sparse and, hence, convenient for computational purposes

To prove the non-singularity of the matrix on the left hand side of equation (16), assume that

$$\begin{pmatrix} K_S + M_S & 0 & C \\ 0 & K_F + M_F & D \\ C^t & D^t & 0 \end{pmatrix} \begin{pmatrix} \tilde{\mathbf{W}}_h \\ \tilde{\mathbf{U}}_h \\ \tilde{\mathbf{P}}_h \end{pmatrix} = \begin{pmatrix} 0 \\ 0 \\ 0 \end{pmatrix}.$$

Matrices $K_S + M_S$ and $K_F + M_F$ are clearly positive definite and hence non-singular. Then

$$(K_S + M_S)\tilde{\mathbf{W}}_h + C\tilde{\mathbf{P}}_h = 0 \Rightarrow \tilde{\mathbf{W}}_h = -(K_S + M_S)^{-1}C\tilde{\mathbf{P}}_h, \tag{17}$$

$$(K_F + M_F)\tilde{\mathbf{U}}_h + D\tilde{\mathbf{P}}_h = 0 \Rightarrow \tilde{\mathbf{U}}_h = -(K_F + M_F)^{-1}D\tilde{\mathbf{P}}_h, \tag{18}$$

and

$$C^t\tilde{\mathbf{W}}_h + D^t\tilde{\mathbf{U}}_h = 0 \Rightarrow -[C^t(K_S + M_S)^{-1}C + D^t(K_F + M_F)^{-1}D]\tilde{\mathbf{P}}_h = 0.$$

Since $K_S + M_S$ and $K_F + M_F$ are positive definite, one has

$$\begin{aligned} 0 &= \tilde{\mathbf{P}}_h^t[C^t(K_S + M_S)^{-1}C + D^t(K_F + M_F)^{-1}D]\tilde{\mathbf{P}}_h \\ &= (C\tilde{\mathbf{P}}_h)^t(K_S + M_S)^{-1}(C\tilde{\mathbf{P}}_h) + (D\tilde{\mathbf{P}}_h)^t(K_F + M_F)^{-1}(D\tilde{\mathbf{P}}_h) \\ &\geqslant \alpha\|C\tilde{\mathbf{P}}_h\|^2 + \beta\|D\tilde{\mathbf{P}}_h\|^2. \end{aligned}$$

Hence $C\tilde{\mathbf{P}}_h = 0$ and $D\tilde{\mathbf{P}}_h = 0$, and so, by using equations (17) and (18), one obtains $\tilde{\mathbf{W}}_h = 0$ and $\tilde{\mathbf{U}}_h = 0$.

Finally, to see that $\tilde{\mathbf{P}}_h = 0$, let P_h be the constant per face function defined on Γ_I having as nodal values the components of the vector $\tilde{\mathbf{P}}_h$. Let us take a function Y_h in the Raviart–Thomas finite element space such that $\mathbf{Y}_h \cdot \mathbf{v} = P_h$. One has

$$0 = \tilde{\mathbf{Y}}_h^t D\tilde{\mathbf{P}}_h = \int_{\Gamma_I} P_h \mathbf{Y}_h \cdot \mathbf{v}\, \mathrm{d}\Gamma = \int_{\Gamma_I} P_h^2\, \mathrm{d}\Gamma, \tag{19}$$

and then $\tilde{\mathbf{P}}_h = 0$. Hence, the matrix on the left hand side of equation (16) is non-singular as claimed.

5. NUMERICAL RESULTS

In this section, numerical results obtained by a FORTRAN implementation of the finite element method described above are presented. This 3D code has been previously validated by computing in plane vibration modes [18] and comparing the results with those obtained with the analogous 2D code of reference [11].

For our numerical experiments three different geometries have been considered: a thick cubic closed vessel (inner edges length 1·00 m, thickness 0·25 m) clamped

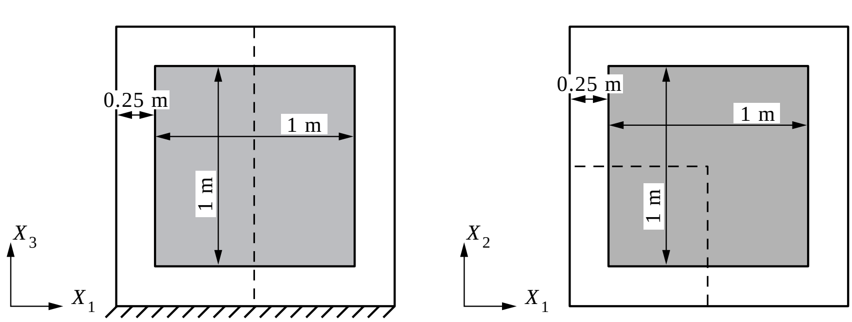

Figure 3. Thick cubic vessel.

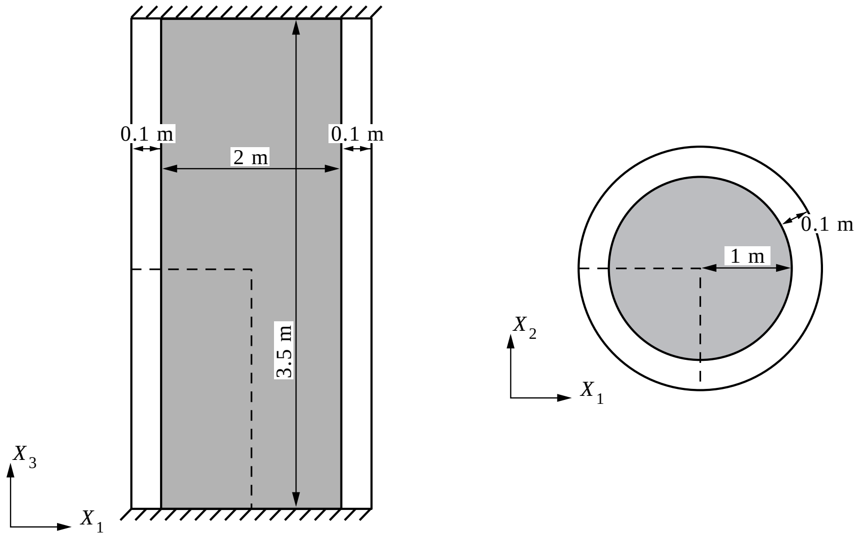

Figure 4. Thin cylinder.

by its bottom and completely filled by the fluid; a thin cylinder (height 3·5 m, inner diameter length 2·0 m, thickness 0·1 m) clamped by both ends and also full of fluid; a cubic cavity (inner edges length 1·00 m) completely filled by the fluid, with all of its walls perfectly rigid except for that on its top which is a clamped plate (thickness 0·05 m). Vertical and horizontal sections are shown in Figure 3 for the cubic vessel, in Figure 4 for the cylinder and in Figure 5 for the rigid cavity covered by a plate. To take advantage of the symmetry, we have considered a quarter of the geometry in the first and third cases and an eighth in the second one, as shown in each figure by the dashed lines.

In all cases steel has been used as the solid with the following physical parameters: density $\rho_s = 7700\ \mathrm{kg/m^3}$, Young's modulus $E = 1{\cdot}44 \times 10^{11}$ Pa, Poisson's coefficient $\nu_s = 0{\cdot}35$, whereas for the fluid we have considered water of density $\rho_F = 1000\ \mathrm{kg/m^3}$, and sound speed $c = 1430$ m/s.

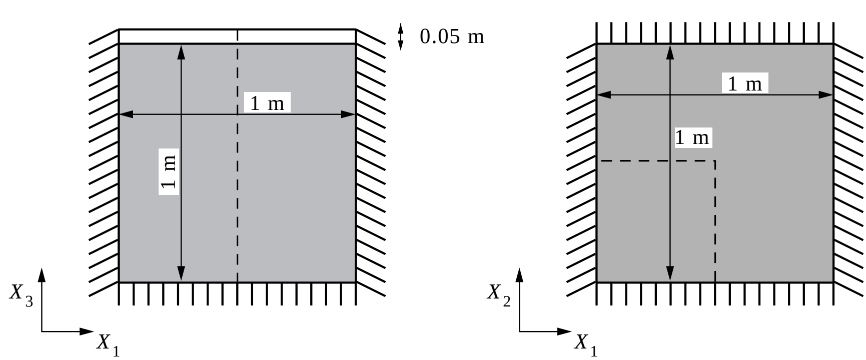

Figure 5. Rigid cavity covered by a plate.

Table 1
Water in a rigid cubic cavity

Mode	Mesh 1	Mesh 2	Mesh 3	Extrapolated	Exact
ω^F_{001}	4482·565	4488·129	4490·046	4492·441	4492·447
ω^F_{100}	4482·652	4488·161	4490·061	4492·439	4492·477
ω^F_{010}	4483·877	4488·842	4490·484	4492·395	4492·477
ω^F_{101}	6356·154	6354·522	6353·999	6353·423	6353·323
ω^F_{110}	6358·052	6355·361	6354·462	6353·400	6353·323
ω^F_{011}	6358·800	6355·627	6354·578	6353·412	6353·323
ω^F_{111}	7803·508	7790·985	7786·666	7781·260	7781·199

Each example has been solved by using differently refined meshes in order to study the convergence behavior of the method. These meshes have been obtained by creating successively refined uniform triangulations of the boundaries and using a general 3D finite element package to generate the tetrahedral meshes in the interior of the domains. For a given mesh, d.o.f. denotes the total number of degrees of freedom (i.e., the sum of those of the solid, the fluid and the interface).

For the first example, three different tetrahedral meshes have been used to discretize a quarter of the thick cubic vessel and the fluid inside: Mesh 1 d.o.f. = 3463 (1575 in the solid, 1696 in the fluid and 192 on the interface); Mesh 2 d.o.f. = 10 498 (4512 in the solid, 5544 in the fluid and 432 on the interface); Mesh 3, d.o.f. = 23 491 (9795 in the solid, 12 928 in the fluid and 768 on the interface).

First, the vibration modes corresponding to the lowest eigenfrequencies of each uncoupled problem have been computed: namely, either the fluid contained in a perfectly rigid solid or the solid without any fluid inside. ω^F_i denotes the eigenfrequencies of the fluid in a rigid cavity and ω^S_i those of the solid *in vacuo*. Each vibration mode of the coupled problem is a perturbation of one of these; thus, the corresponding eigenfrequencies are denoted either by ω^F_i or ω^S_i, according to which they are a perturbation of, and are called, "fluid" or "solid" eigenmodes, respectively.

For the fluid in a rigid cavity, the computed vibration frequencies are compared with the exact ones which, in this case, are analytically known; in fact, for a cubic cavity with inner edges of length L, the free vibration angular frequencies are

$$\omega^F_{lmn} = (c\pi/L)\sqrt{l^2 + m^2 + n^2}, \qquad l, m, n = 0, 1, 2, \ldots, \qquad l + m + n \neq 0,$$

with corresponding pressure amplitudes

$$P(x_1, x_2, x_3) = \cos(l\pi x_1/L)\cos(m\pi x_2/L)\cos(n\pi x_3/L), \qquad 0 < x_1, x_2, x_3 < L.$$

Table 1 shows the values of the lowest eigenfrequencies (in rad/s) computed with each mesh and the more accurate approximation that is obtained by extrapolating them. The table also includes the corresponding exact vibration frequencies.

Notice that the values obtained by extrapolating the results on these three meshes agree with the exact ones almost with five significant digits.

TABLE 2

"Fluid" elastoacoustic and uncoupled (rigid cavity) modes for a cubic vessel

	Steel vessel			Rigid cavity
Mode	Mesh 1	Mesh 2	Mesh 3	Mesh 3
ω^F_{001}	4619·454	4571·933	4579·967	4490·046
ω^F_{100}	4238·184	4193·331	4163·331	4163·296
ω^F_{010}	4231·182	4186·356	4158·101	4490·484
ω^F_{101}	5906·880	5717·052	5603·941	6353·999
ω^F_{110}	6150·860	6036·036	5984·662	6354·462
ω^F_{011}	5896·335	5716·762	5603·425	6354·578
ω^F_{111}	7558·874	7487·871	7748·380	7786·666

On the other hand, because of the symmetry of the geometry, the two lowest exact vibration frequencies has multiplicity 3. However, since the meshes have been created by a general 3D generator, they do not preserve this symmetry and hence the corresponding computed frequencies differ slightly.

Note also that the first three frequencies converge from below, while the next three converge from above. This is something typical of displacement formulations (see, for instance, Table 1 in reference [13]); it is due to the fact that the lowest eigenvalue of the mathematical problem is zero with infinite multiplicity and, because of this, the *min–max* principles yielding convergence from above in other vibration problems do not apply in this case.

Table 2 shows the computed lowest eigenfrequencies of the "fluid" modes for the coupled problem: water contained in the steel cavity. The corresponding uncoupled eigenfrequencies (i.e., within a perfectly rigid cavity) computed on the finest mesh are also included to appreciate the effect of the elastic response of the solid walls.

Note that the computed values of the first eigenfrequency in Table 2 do not behave monotonically as with all the other modes. This is due to a resonance effect with the "solid" eigenmode ω^S_6 in Table 3. In fact, both vibration modes have the

TABLE 3

"Solid" coupled and uncoupled (in vacuo) modes for a cubic steel vessel

	Filled with water			*In vacuo*
Mode	Mesh 1	Mesh 2	Mesh 3	Mesh 3
ω^S_1	1624·671	1581·248	1563·084	1595·985
ω^S_2	2598·815	2531·345	2503·574	2507·669
ω^S_3	3631·327	3532·999	3477·217	3717·577
ω^S_4	5036·372	4969·426	4937·061	4626·765
ω^S_5	4728·898	4565·646	4483·854	4677·719
ω^S_6	4896·822	4595·293	4414·306	4786·102

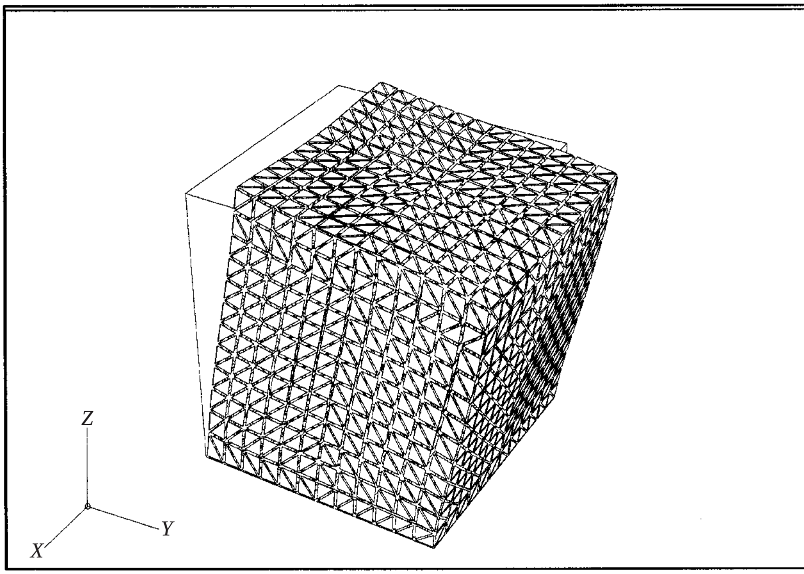

Figure 6. Cube, mode ω_1^S; deformed structure.

same symmetry and very close frequencies. This is particularly true for the values computed on Mesh 2 and hence, because of the typical "veering" phenomenon (see reference [1]), these values tend to separate from each other.

Table 3 shows analogous results to those of Table 2 for the "solid" vibration modes. Note that, for the solid *in vacuo*, the method reduces to the classical computation with four-node linear tetrahedral elements.

The good convergence observed in these tables shows that the lowest elastoacoustic vibration modes can be reliably computed with this method.

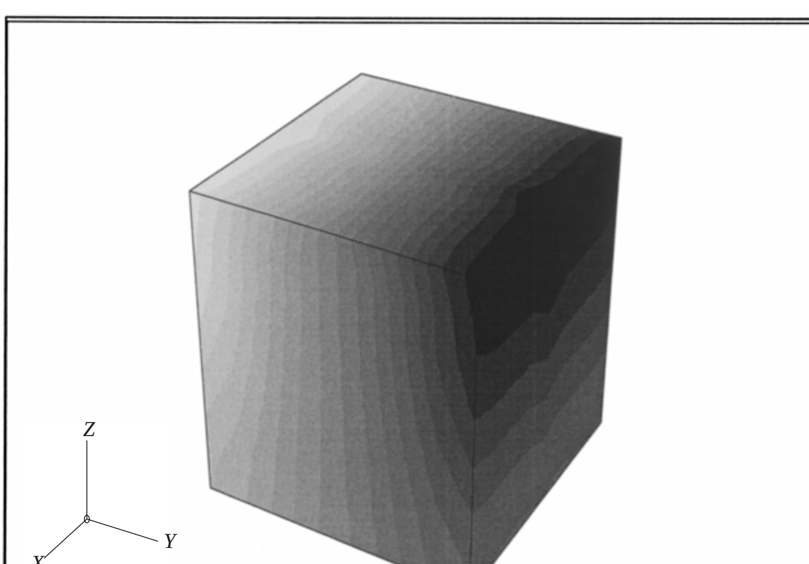

Figure 7. Cube, mode ω_1^S; pressure in the fluid.

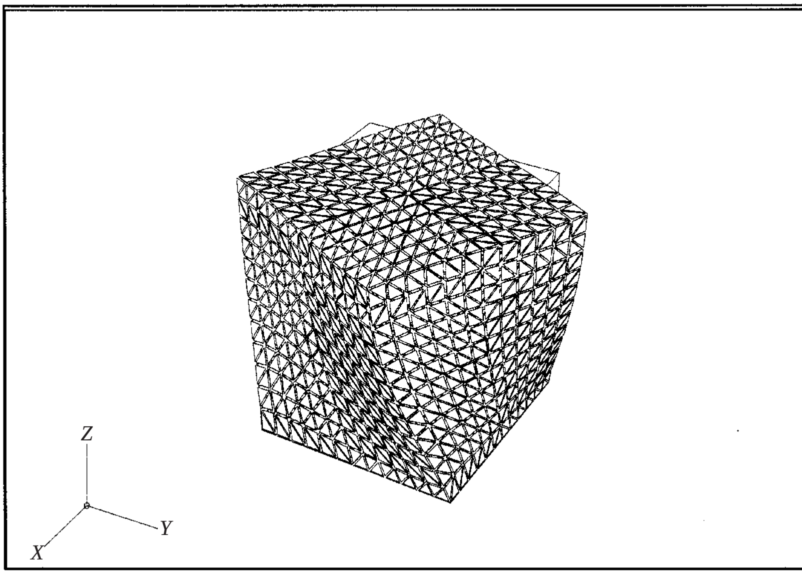

Figure 8. Cube, mode ω_2^S; deformed structure.

This example is concluded by showing in Figures 6–11 the deformed structure and the fluid pressure field for three vibration modes of the coupled problem.

For the second example, the previous steps have been repeated with the thin cylinder. Note that this case is not covered by the theory in reference [18] since the solid is not polyhedral. However, the numerical results below show that the performance of the method is as good as for polyhedral geometries.

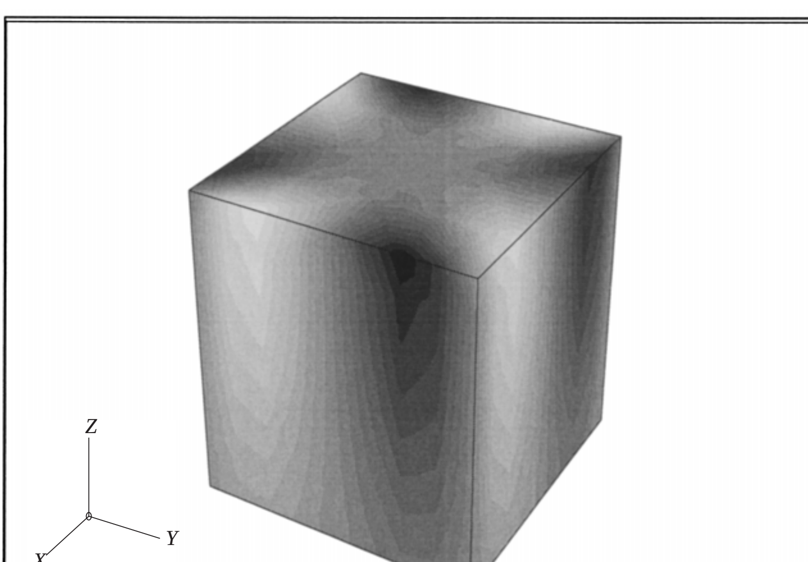

Figure 9. Cube, mode ω_2^S; pressure in fluid.

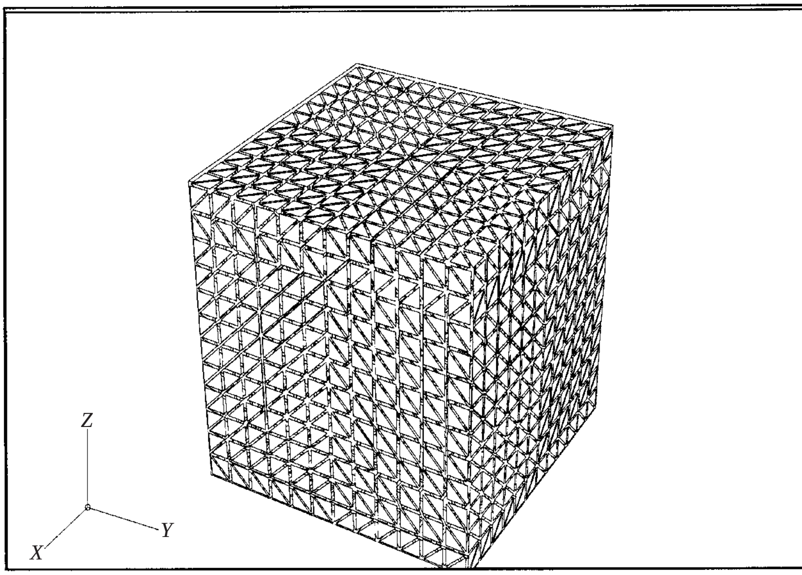

Figure 10. Cube, mode ω^F_{001}; deformed structure.

Again three increasingly refined meshes have been used for the eighth of the cylinder and the fluid inside: Mesh 1, d.o.f. = 1068 (240 in the solid, 772 in the fluid and 56 on the interface); Mesh 2, d.o.f. = 7215 (1215 in the solid, 5776 in the fluid and 224 on the interface); Mesh 3, d.o.f. = 22 980 (3432 in the solid, 19 044 in the fluid and 504 on the interface).

The exact eigenmodes for the uncoupled problem of a fluid contained in a cylindrical rigid cavity can be also analytically computed; the free vibration angular frequencies are given in this case by

$$\omega^F_{lnm} = \begin{cases} \dfrac{c\pi l}{H}, & n = m = 0, \qquad l = 1, 2, 3, \ldots \\[2ex] c\sqrt{\dfrac{\pi^2 l^2}{H^2} + \dfrac{\zeta^2_{nm}}{R^2}}, & l, n = 0, 1, 2, \ldots, \quad m = 1, 2, \ldots \end{cases},$$

where R and H are the radius and the height of the cylinder (in our case $R = 1$ m and $H = 3{\cdot}5$ m) and ζ_{nm} is the mth positive root of the derivative of the first kind Bessel function $\mathrm{J}_n(\zeta)$.

Table 4 shows that the convergence for the vibration modes of the fluid is excellent.

Table 5 shows the computed frequencies of the "fluid" modes for water contained in the thin steel cylinder. Once more the convergence is very good. As in Table 2, the corresponding uncoupled modes computed with the finest mesh are also included for comparison.

The eigenfrequencies of three vibration "solid" modes of the cylinder filled with water and *in vacuo* have also been computed.

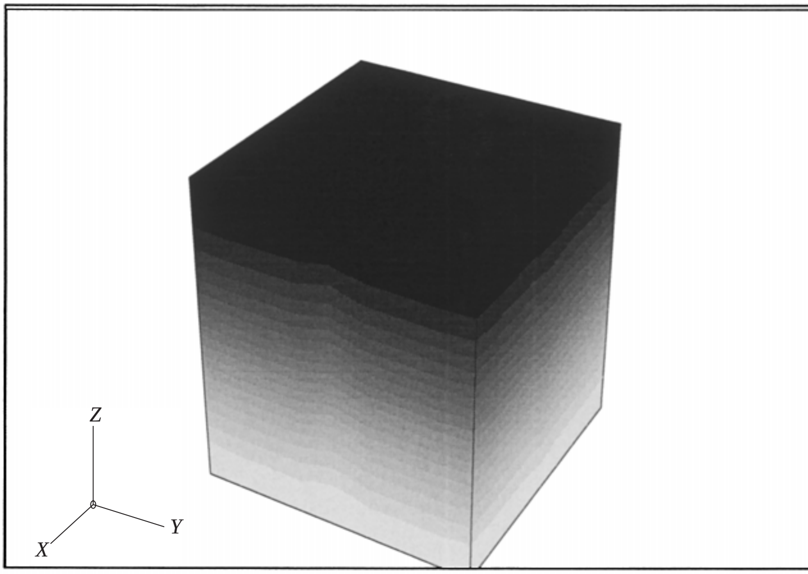

Figure 11. Cube, mode ω^F_{001}; pressure in the fluid.

The poor performance observed in Table 6, namely the large variations between the eigenfrequencies computed with each mesh (in particular for ω^S_1 and ω^S_3), is a defect neither of the elements used for the fluid nor of the methodology proposed to impose the kinematic constraints. In fact, for the uncoupled problem of the cylinder *in vacuo* these variation are equally large and, in this case our method

TABLE 4

Water in a rigid cylindrical cavity

Mode	Mesh 1	Mesh 2	Mesh 3	Extrapolated	Exact
ω^F_{100}	1282·048	1283·184	1283·396	1283·567	1283·565
ω^F_{200}	2554·990	2564·085	2565·777	2567·139	2567·130
ω^F_{011}	2670·045	2642·217	2637·051	2632·906	2632·916
ω^F_{111}	2964·963	2937·717	2932·893	2929·238	2929·127

TABLE 5

"Fluid" elastoacoustic and uncoupled (rigid cavity) modes for a cylindrical vessel

	Steel vessel			
Mode	Mesh 1	Mesh 2	Mesh 3	Rigid cavity Mesh 3
ω^F_{100}	1188·443	1166·649	1158·687	1283·396
ω^F_{200}	2348·552	2281·999	2255·354	2565·777
ω^F_{011}	2948·532	2775·609	2695·288	2637·051
ω^F_{111}	2338·165	2142·013	2085·688	2932·893

TABLE 6

"Solid" coupled and uncoupled (in vacuo) modes for a cylindrical steel vessel

	Filled with water			*In vacuo*		
Mode	Mesh 1	Mesh 2	Mesh 3	Mesh 1	Mesh 2	Mesh 3
ω_1^S	1701·500	1153·671	1009·377	2089·007	1409·556	1232·094
ω_2^S	1311·843	1237·666	1219·264	1745·492	1648·411	1624·648
ω_3^S	4003·714	2291·144	1707·784	4833·060	2697·915	2001·229

Table 5 shows the computed frequencies of the "fluid" modes for water contained in the thin steel cylinder. Once more the convergence is very good. As in Table 2, the corresponding uncoupled modes computed with the finest mesh are also included for comparison.

The eigenfrequencies of three vibration "solid" modes of the cylinder filled with water and *in vacuo* have also been computed.

The poor performance observed in Table 6, namely the large variations between the eigenfrequencies computed with each mesh (in particular for ω_1^S and ω_3^S), is a defect neither of the elements used for the fluid nor of the methodology proposed to impose the kinematic constraints. In fact, for the uncoupled problem of the cylinder *in vacuo* these variation are equally large and, in this case our method reduces to compute the vibration modes of the structure by classical four-node tetrahedral elements. These results clearly show the need for combining Raviart–Thomas elements for the fluid with adequate 2D models of thin structures as is done below in the case of a plate.

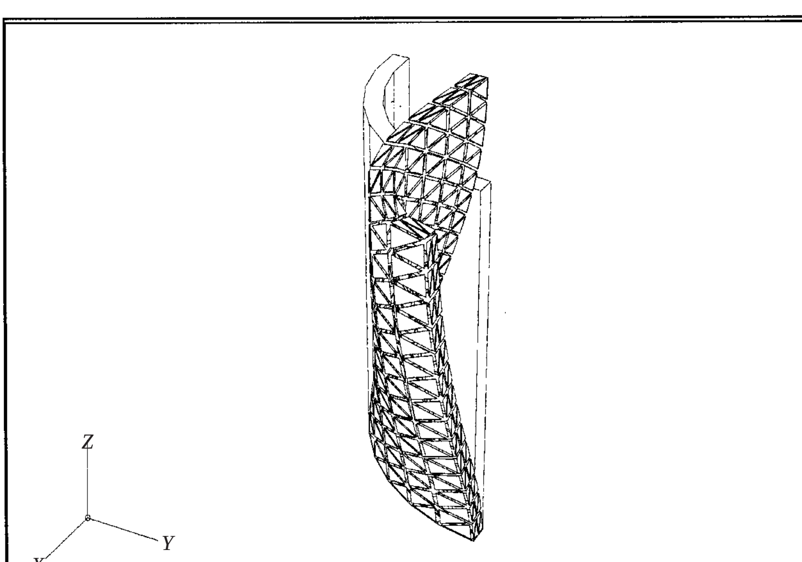

Figure 12. Eighth of the cylinder, mode ω_1^S; deformed structure.

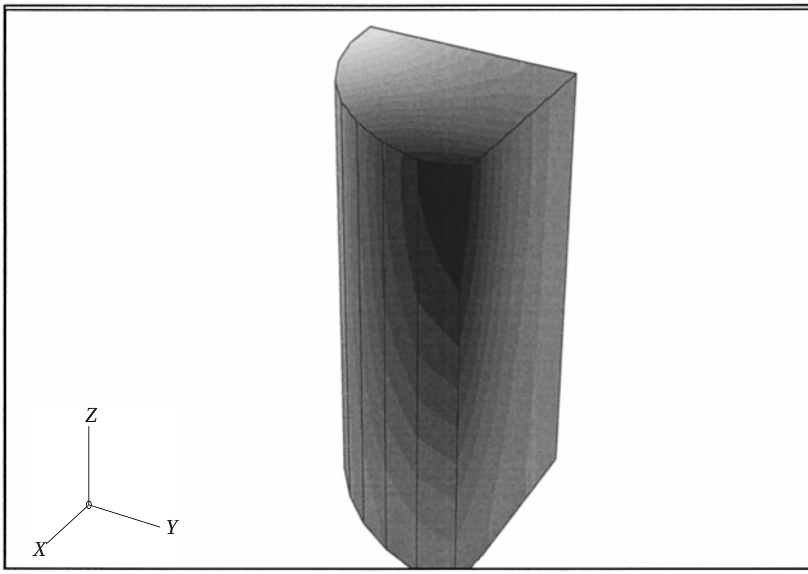

Figure 13. Eighth of the cylinder, mode ω_1^S; pressure in the fluid.

This example is concluded by showing in Figures 12–17 one-eighth of the deformed cylinder and the fluid pressure field for three modes of this coupled problem.

The third problem considered consists of computing the vibration modes of a plate in contact with a fluid. The Reissner–Mindlin model was used for the bending of the plate, discretized by *MITC*3, a locking free finite element method introduced by Bathe and Dvorkin [19]. In this method, the transversal displacements of the

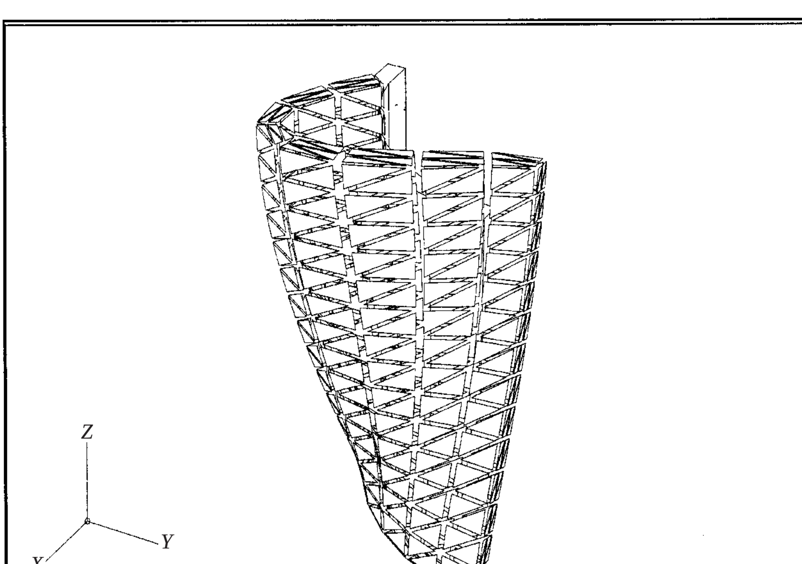

Figure 14. Eighth of the cylinder, mode ω_2^S; deformed structure.

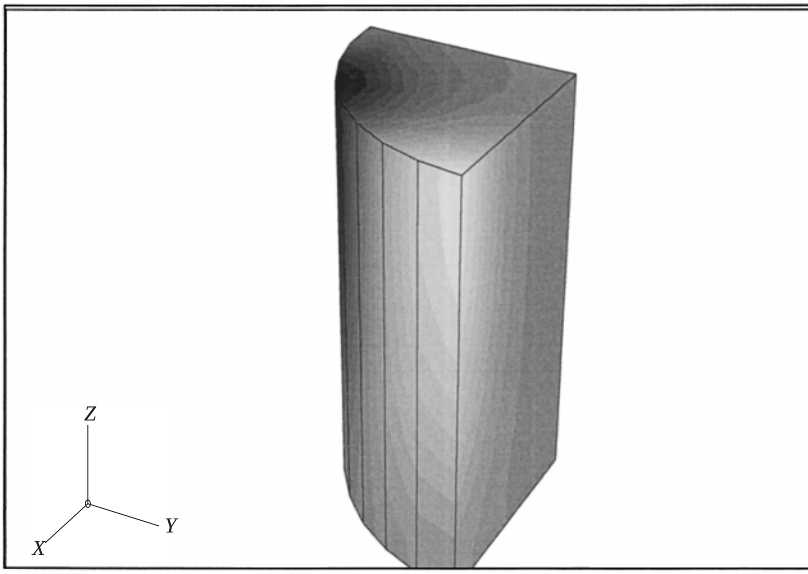

Figure 15. Eighth of the cylinder, mode ω_2^S; pressure in the fluid.

plate are discretized by piecewise linear functions which have been coupled with Raviart–Thomas elements for the fluid displacements, as in the examples above. A thorough theoretical analysis of this problem can be found in reference [20], where it is proved that the coupled method does not lock as the plate thickness becomes small and hence that it can be reliably used no matter how thin the plate is.

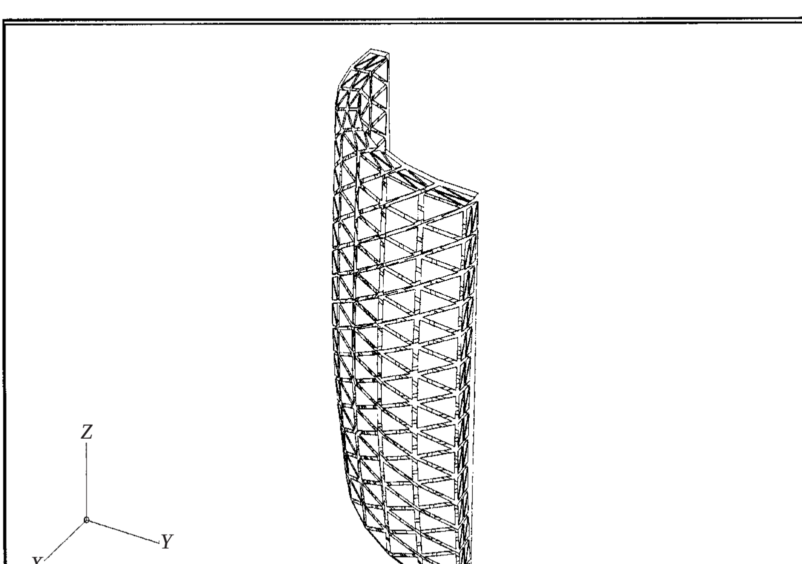

Figure 16. Eighth of the cylinder, mode ω_{100}^F; deformed structure.

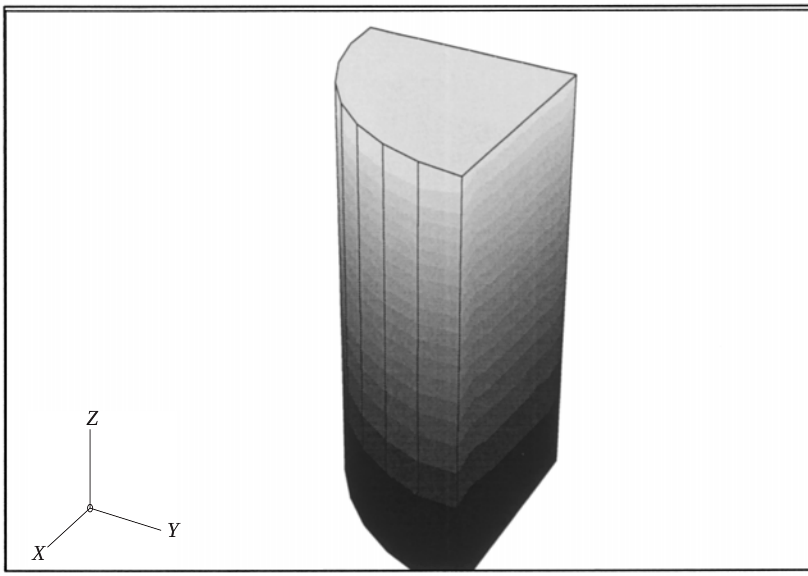

Figure 17. Eighth of the cylinder, mode ω^F_{100}; pressure in the fluid.

Once more, three differently refined meshes have been used: Mesh 1, d.o.f. = 1859 (131 in the plate, 1696 in the fluid and 32 on the interface); Mesh 2, d.o.f. = 5883 (267 in the plate, 5544 in the fluid and 72 on the interface); Mesh 3, d.o.f. = 13 507 (451 in the plate, 12 928 in the fluid and 128 on the interface).

TABLE 7

Elastoacoustic and uncoupled modes for a plate–fluid system

	Plate–fluid coupled modes			Uncoupled modes
Mode	Mesh 1	Mesh 2	Mesh 3	Mesh 3
ω^S_1	2177·939	2170·651	2167·922	2327·212
ω^F_{001}	4890·610	4854·706	4841·131	4490·046
ω^F_{100}	4885·135	4857·721	4847·314	4490·061
ω^F_{010}	4884·680	4857·568	4847·249	4490·484
ω^S_2	3545·822	3525·596	3518·040	4689·178
ω^S_3	3547·250	3526·172	3518·343	4689·178
ω^F_{101}	6758·293	6694·080	6669·856	6353·999
ω^F_{110}	6726·668	6675·258	6656·259	6354·462
ω^F_{011}	6758·265	6694·111	6669·870	6354·578
ω^S_4	5529·026	5449·373	5418·194	6826·651
ω^F_{111}	8273·536	8175·172	8138·963	7786·666
ω^S_5	6943·492	6866·441	6831·714	8197·654
ω^S_6	7741·467	7465·741	7355·582	8374·716

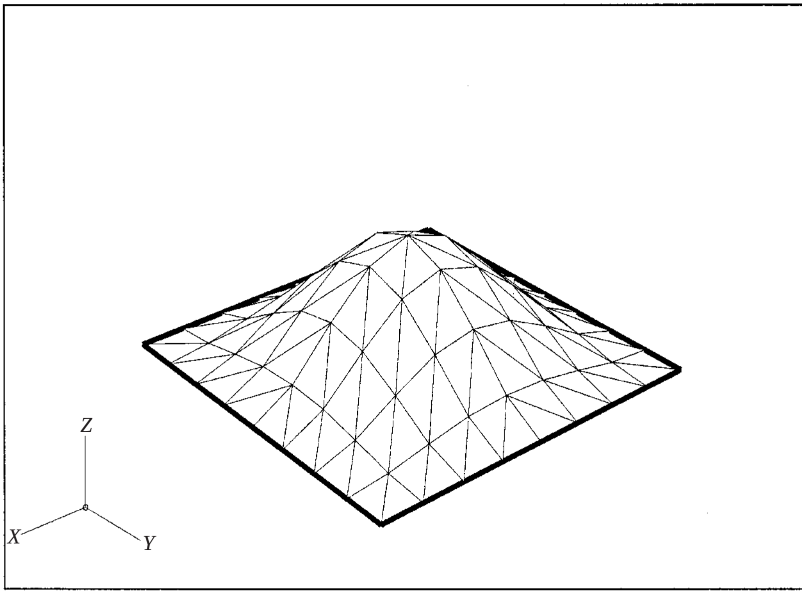

Figure 18. Fluid–plate, mode ω_1^S; deformed structure.

Table 7 shows the computed lowest frequencies of the coupled system. Also included are the frequencies of the corresponding uncoupled modes for comparison. The table shows the excellent performance of the method.

Finally, Figures 18–23 show the deformed plate and the pressure field for some vibration modes in the previous table.

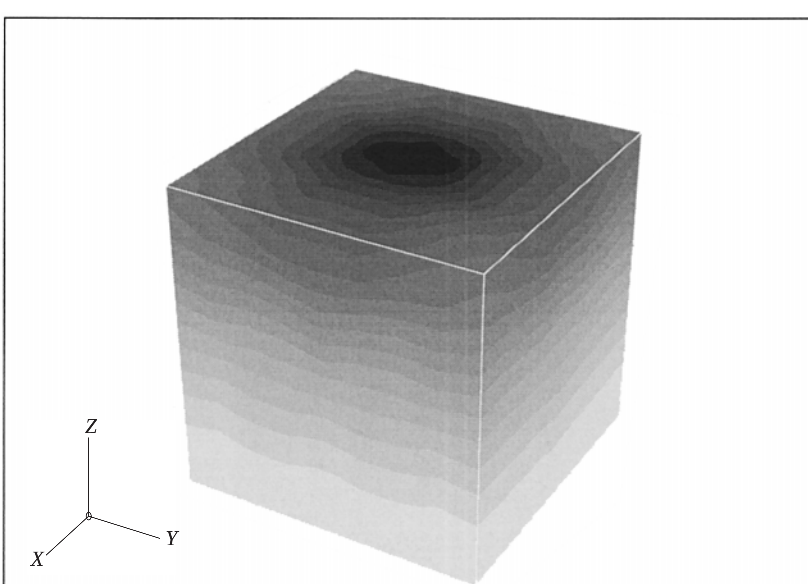

Figure 19. Fluid–plate, mode ω_1^S; pressure in the fluid.

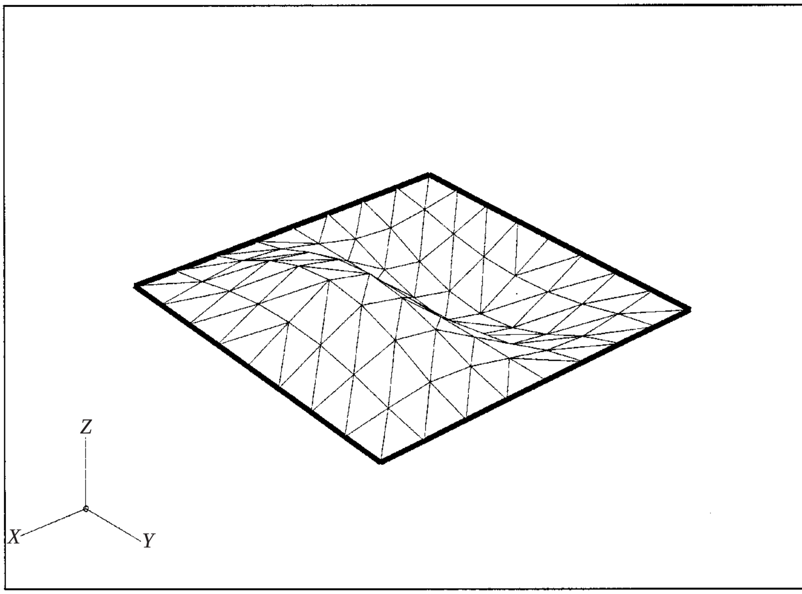

Figure 20. Fluid–plate, mode ω_2^S; deformed structure.

6. CONCLUSIONS

In this paper a finite element method has been proposed to solve 3D elastoacoustic spectral problems. It involves a formulation where the fluid as well as the solid are described by their displacement fields. The main advantage with respect to standard finite element methods is that it yields symmetric sparse eigenvalue problems without introducing numerical spurious eigenmodes.

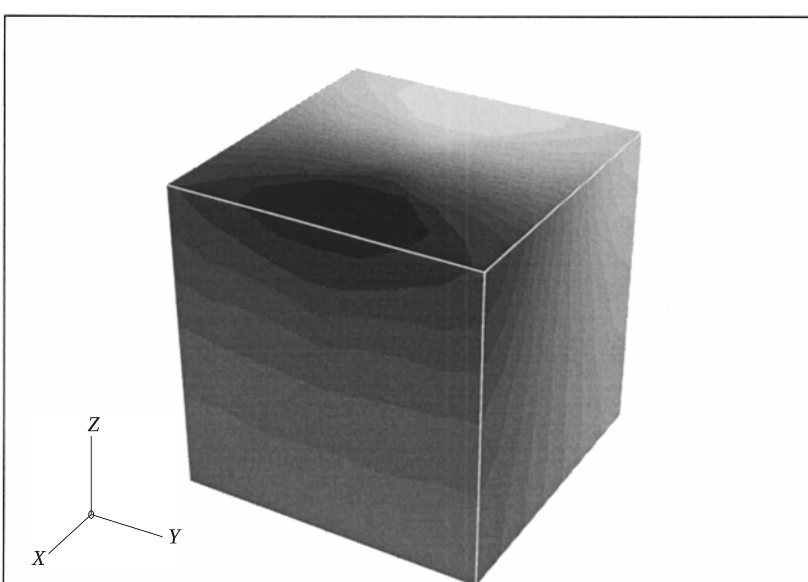

Figure 21. Fluid–plate, mode ω_2^S; pressure in the fluid.

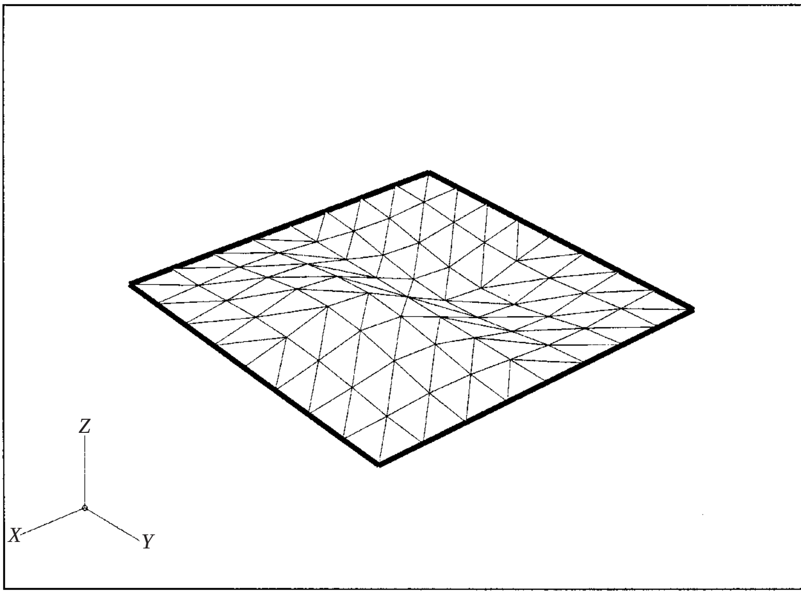

Figure 22. Fluid–plate, mode ω^F_{100}; deformed structure.

Moreover the coupling conditions on the fluid–solid interface are very easily imposed by using the interface pressure as a Lagrange multiplier, allowing eventually the use of non-compatible fluid and solid meshes.

For a given mesh, the present method is more expensive in terms of degrees of freedom if compared to other symmetric methods based on pressure/potential formulations for the fluid or to unsymmetric methods based on pressure

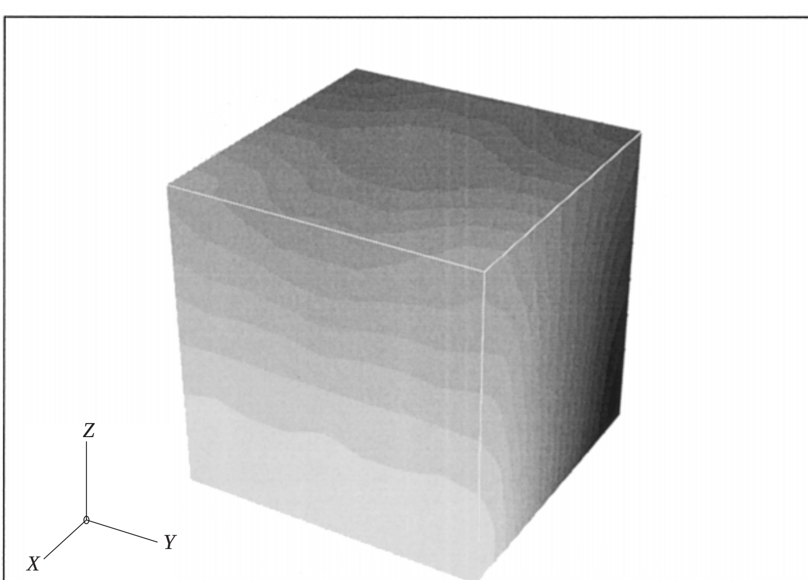

Figure 23. Fluid–plate, mode ω^F_{100}; pressure in the fluid.

formulations. However, the matrices obtained with Raviart–Thomas elements are much more sparse than those of these other methods: they have at most seven non null entries per row versus around 20 for four-node tetrahedral elements. Therefore, the overall computational cost could be significantly reduced if iterative methods based on matrix vector multiplications are used to solve the eigenproblems.

ACKNOWLEDGMENTS

This work was partially supported by FONDECYT (Chile) through its grant no. 1.960.615, Instituto de Cooperación Iberoamericana (ICI, Spain) and Proyecto de Colaboración Hispano Francesa through grant nos. HF1996-0172 and HF1997-0194.

REFERENCES

1. H. J.-P. Morand and R. Ohayon 1992 *Interactions Fluides–Structure*. Paris: Masson.
2. C. Conca, J. Planchard and M. Vanninathan 1992 *Fluids and Periodic Structures*. Paris: Masson.
3. O. C. Zienkiewicz and R. L. Taylor 1991 *The Finite Element Method*, Volume 2. London: McGraw–Hill.
4. M. Petyt, J. Lea and G. H. Koopmann 1976 *Journal of Sound and Vibration* **45**, 495–502. A finite element method for determining the acoustic modes of irregular shaped cavities.
5. G. C. Everstine 1981 *Journal of Sound and Vibration* **79**, 157–160. A symmetric potential formulation for fluid–structure interaction.
6. H. Morand and R. Ohayon 1979 *International Journal for Numerical Methods in Engineering* **14**, 741–755. Substructure variational analysis of the vibrations of coupled fluid–structure systems. Finite element results.
7. K. J. Bathe, C. Nitikitpaiboon and X. Wang 1995 *Computers and Structures* **56**, 225–237. A mixed displacement-based finite element formulation for acoustic fluid–structure interaction.
8. X. Wang and K. J. Bathe 1997 *International Journal for Numerical Methods in Engineering* **40**, 2001–2017. Displacement/pressure based mixed finite element formulations for acoustic fluid–structure interaction problems.
9. L. Kiefling and G. C. Feng 1976 *American Institute of Aeronautics and Astronautics Journal* **14**, 199–203. Fluid–structure finite element vibration analysis.
10. M. Hamdi, Y. Ousset and G. Verchery 1978 *International Journal for Numerical Methods in Engineering* **13**, 139–150. A displacement method for the analysis of vibrations of coupled fluid–structure systems.
11. A. Bermúdez and R. Rodríguez 1994 *Computer Methods in Applied Mechanics and Engineering* **119**, 355–370. Finite element computation of the vibration modes of a fluid–solid system.
12. L. G. Olson and K. J. Bathe 1983 *Nuclear Engineering and Design* **76**, 137–151. A study of displacement-based fluid finite elements for calculating frequencies of fluid and fluid–structure systems.
13. H. C. Chen and R. L. Taylor 1990 *International Journal for Numerical Methods in Engineering* **29**, 683–698. Vibration analysis of fluid–solid systems using a finite element displacement formulation.

14. A. Bermúdez, R. Durán, M. A. Muschietti, R. Rodríguez and J. Solomin 1995 *Society for Industrial and Applied Mathematics Journal on Numerical Analysis* **32**, 1280–1295. Finite element vibration analysis of fluid–solid systems without spurious modes.
15. P. A. Raviart and J. M. Thomas 1972 in *Mathematical Aspects of Finite Element Methods*. Lecture Notes in Mathematics Volume 606, Berlin: Springer-Verlag, 292–315. A mixed finite element method for second order elliptic problems.
16. L. D. Landau and E. M. Lifshitz 1959 *Theory of Elasticity*. Oxford: Pergamon Press.
17. F. Brezzi and M. Fortin 1991 *Mixed and Hybrid Finite Element Methods*. New York: Springer-Verlag.
18. A. Bermúdez, L. Hervella-Nieto and R. Rodríguez 1996 in *Numerical Methods in Engineering* '96. New York: J. Wiley & Sons, 874–880. Numerical solution of three-dimensional elastoacoustic problems.
19. K. J. Bathe and E. N. Dvorkin 1985 *International Journal for Numerical Methods in Engineering* **21**, 367–383. A four-node plate bending element based on Mindlin/Reissner plate theory and a mixed interpolation.
20. R. Durán, L. Hervella-Nieto, E. Liberman, R. Rodríguez and J. Solomin 1998 Finite element analysis of the vibration problem of a plate coupled with a fluid (submitted).